Reaction mechanism and isotope effects derived from centroid transition state theory in intramolecular proton transfer reactions

Radu Iftimie and Jeremy Schofield
Chemical Physics Theory Group, Department of Chemistry, University of Toronto, Toronto, Ontario, Canada M5S 3H6

(Received 19 April 2001; accepted 12 July 2001)

In this article the tautomerization reaction of the enol form of malonaldehyde is used to investigate the magnitude and origin of changes in centroid transition state theory proton transfer reaction rate predictions caused by the quantum dispersion of heavy nuclei. Using an empirical valence bond method to construct the potential energy surface, it is found that quantization of the nuclear degrees of freedom of the carbon atoms significantly influences the centroid potential of mean force used to describe the proton transfer reaction. In contrast, an *ab initio* simulation carried out using a recently developed molecular mechanics based importance sampling method [J. Chem. Phys. **114**, 6763 (2001)] in combination with an accurate density functional theory evaluation of the electronic energies shows a substantially smaller influence of the quantum nuclear degrees of freedom of the secondary atoms on the centroid potential of mean force. A detailed analysis of the different influence of quantization of the nuclear degrees of freedom of secondary atoms observed in the *ab initio* and empirical valence bond centroid potential of mean force was carried out. It is shown that for the empirical valence bond potential, a significant decrease of the centroid potential of mean force arises through the quantum tunneling of carbon atoms in the molecular backbone. Furthermore, it is demonstrated that in molecular mechanics potentials aimed to describe intramolecular proton transfer reactions, the functional form of the potential energy terms coupling the primary and secondary atom motions as the reaction proceeds as well as the mass of the primary particle can significantly influence the centroid transition state theory predictions of secondary kinetic isotope effects. Finally, the dependence of the reaction rate predictions and isotope effects on the choice of reaction coordinate is investigated and the validity of calculating kinetic isotope effects using the centroid transition state theory formalism is discussed. © *2001 American Institute of Physics.* [DOI: 10.1063/1.1399060]

I. INTRODUCTION

One of the most interesting aspects of intramolecular proton transfer processes is the nature in which structural rearrangements involving the proton are correlated with topological changes in the rest of the molecule as the reaction proceeds. Since these correlations reflect the reaction mechanism, study of the connection between the motion of the proton and the remaining degrees of freedom can provide valuable insight into how a reaction proceeds. The correlations between the molecular motions can be probed by examining the changes in reaction rate caused by isotopic substitution at different atomic centers. The ratios of observed reaction rates for different isotopic compositions of the chemical species are generally known as kinetic isotope effects. Because kinetic isotope effects reflect the nature of bonding in the vicinity of the labeled atoms, they provide useful information about the chronological sequence of changes in the bonding structure. Kinetic isotope effects are typically differentiated by the location of the isotopic substitution relative to the atoms involved in bond-breaking and bond-forming events: *Primary* kinetic isotope effects arise due to isotopic substitution at an atomic position in which the labeled atom is directly involved in chemical bond-breaking or bond-forming, whereas *secondary* kinetic isotope effects occur at atomic centers which are anticipated to play a peripheral role in the reaction. Studies involving kinetic measurements in experiments where both primary and secondary positions are isotopically substituted are particularly helpful in predicting the reaction mechanism and have been used extensively in the physical organic chemistry literature.[1]

However, experimental studies of kinetic isotope effects are limited by the relatively small number of naturally-occurring isotopes and by the difficulty of synthesizing chemical species with a particular isotopic labeling. Computational studies of isotope effects, on the other hand, allow fictitious as well as naturally-occurring isotopic changes which permit more appreciable kinetic isotope effects to be obtained. Unfortunately, the accuracy of numerical calculations of isotope effects depends greatly on the method used to calculate energies of different molecular configurations. Although accurate predictions of equilibrium and transition state structures and energies are possible using *ab initio* methods, the computational demand of *ab initio* methods limits the size of the systems which can be analyzed to molecules containing at best several dozens of atoms. One way of extending the size of systems which can be studied with reasonable accuracy consists of constructing realistic mo-

lecular mechanics potentials carefully parameterized using *ab initio* electronic structure methods. A clear advantage of utilizing an accurate molecular mechanics potential is the ease of interpreting the way in which a particular type of interaction or term in the potential affects the magnitude of kinetic isotope effects. In addition, the relation between particular terms in the potential and the reaction mechanism can be probed which sheds light onto the connection between reaction mechanism and isotope effects. A detailed understanding of this connection from simulation is important since it can be obtained only indirectly from experimental studies.

A practical way to estimate kinetic isotope effects consists of using (quantum) transition state theories to predict reaction rates by studying the changes in the potential of mean force at the dividing surface due to isotopic substitutions. One of the most intriguing results in recent studies of intramolecular proton transfer reactions demonstrates that quantum dispersion effects of the nuclei of heavy atoms have considerable influence on the magnitude of the centroid potential of mean force describing the tautomerization reaction in acetylacetone.[2] These results suggest that it is essential to treat the quantum behavior of the nuclei of particular secondary atoms in order to obtain accurate reaction rates for some proton-transfer reactions within a centroid transition state theory framework. It is therefore compelling to investigate how choice of reaction coordinate and details of the potential energy surface determine the increased importance of the nuclear dispersion of heavy nuclei on the centroid potential of mean force.

In the article, the influence of the quantum nuclear degrees of freedom of secondary atomic centers is examined using both molecular mechanics and *ab initio* electronic structure methods in combination with imaginary-time path-integral simulation techniques. In this study, the intramolecular transfer is considered to occur in a core region of a molecule which is taken to have a structure similar to malonaldehyde. Because unimolecular reaction rate descriptions of the gas-phase tautomerization reaction in malonaldehyde are not appropriate due to the small size of the molecular system and long quantum coherence time of the dynamics[3], the potential of mean force calculations carried out here cannot be interpreted in terms of rate constant predictions for the proton transfer reaction in malonaldehyde. Because the influence of the solvent is neglected in our calculations of the potential of mean force, one might expect some differences between our results and those that would be obtained in an actual calculation of the system in a condensed-phase environment. However, it seems reasonable to assume that the solvent has little influence on secondary kinetic isotope effects in intramolecular proton transfer reactions[1]. Under these assumptions, the qualitative features pertaining to the influence of the quantum nuclear degrees of freedom of the secondary atoms on the centroid potential of mean force of malonaldehyde should provide insight into real kinetic isotope effects in some intramolecular proton transfer reactions for which unimolecular rate descriptions are appropriate.

In Sec. II, a brief review of centroid quantum transition state theory for activated processes[4,5] together with the molecular mechanics based importance function (MMBIF) simulation approach[6] are reviewed. In Sec. III, the centroid potential of mean force obtained using *ab initio* electronic structure methods are contrasted with results obtained using an ad hoc molecular mechanics empirical valence bond potential (EVB).[7] A bond evolution theory[8,9] molecular mechanics potential is constructed such that continuous changes in the potential surface corresponding to changes in the reaction mechanism induce variable secondary atom isotope effects in the centroid potential of mean force calculations. The results obtained utilizing the bond evolution theory potential are used to investigate the qualitative features of the *ab initio* and EVB potentials responsible for the observed differences in the centroid potential of mean force in the two systems as well as how these features influence the reaction mechanism. The potential of mean force and reaction rates are computed and contrasted using different choices of reaction coordinate in order to understand the limitations of centroid transition state theory calculations in predicting real kinetic isotope effects. Several intriguing aspects of the isotope effects obtained using mixed isotopic labeling at both primary and secondary positions with the EVB potential are interpreted in the context of semiclassical transition state theory. The analysis suggests that tunneling of heavy atoms at secondary positions could be an important aspect in some intramolecular proton transfer reactions. Conclusions and implications of this work are discussed in Sec. IV.

II. THEORETICAL BACKGROUND AND COMPUTATIONAL APPROACH

A. Centroid quantum transition state theory

Classical rate theory is a well-established subject and a number of excellent reviews of the subject have appeared in the literature.[10] The conditions needed for a valid description of a chemical reaction in terms of mass action kinetic equations have been largely understood.[11] These requirements consist essentially of the separation of the time scale characterizing the reactive process from the other time scales in the system.[10]

Assuming that a dividing surface can be identified which separates the reactant subspace of configurational space from the product subspace such that all dynamical trajectories started at this surface end up in the subspace toward which they were initially directed, one can write the transition state (TST) expression for the reaction rate[2,6] as

$$k_{\mathrm{TST}} = \sqrt{\frac{k_B T}{2\pi m_{\mathrm{eff}}}} \frac{\exp(-\phi(0)/k_B T)}{\int_0^\infty dq \exp(-\phi(q)/k_B T)}. \tag{1}$$

The first ratio in the product on the right-hand side of Eq. (1) represents a kinetic prefactor obtained from integration over the momenta of the system. The reaction coordinate $q(\mathbf{x})$ characterizes the dynamics of the transition between the reactant and the product, and is defined such that $q(\mathbf{x})=0$ is the equation for the dividing surface necessary in the TST formulation. The mass m_{eff} is an ''effective mass'' for motion along the reaction coordinate, and is defined by

$$m_{\mathrm{eff}}=\left\langle \sqrt{\sum \frac{1}{m_i}\left(\frac{\partial q}{\partial x_i}\right)^2}\right\rangle_{(q=0)}^{-2}, \tag{2}$$

where the configurational average $\langle\cdots\rangle$ in Eq. (2) is a constrained average performed only at the dividing surface. In Eq. (1), $\phi(q)=-k_BT\ln\langle\delta(q(\mathbf{x})-q)\rangle$ is defined to be the potential of mean force at reaction coordinate value q, where k_B is Boltzmann's constant and T is the absolute temperature.

Chemical reactions can be understood in the framework of classical mechanics as thermally activated transitions between two minima on the potential energy surface. In order for a particle obeying the laws of the classical mechanics to transfer from one minimum on the potential energy surface to another minimum, the particle must acquire enough energy to visit the transition state region during its dynamics. The description of chemical reactions as a semiclassical or quantum mechanical process is considerably more difficult since quantized vibrational motions can have a considerable influence on the reaction and a quantum particle can tunnel through a potential barrier as the reaction proceeds. The nature of quantum dynamics leads to an additional requirement in order for a chemical reaction to be described as a first-order kinetic process: an efficient mechanism must exist which leads to the rapid phase decoherence of the wave functions localized in the reactant and product wells on a time scale which is smaller than the reactive time scale.

Much recent work in the development of quantum rate formalisms has focused on generalizing and extending classical TST to the case of quantum many-body systems. A purely statistical quantum transition state theory, which does not require calculation of the explicit time evolution of the system, is particularly useful for analyzing ''rare events'' such as chemical transformations since accurate calculations of quantum dynamics can presently be carried out only for low-dimensional systems and short time intervals. Several versions of quantum transition state theory have been proposed.[12] One of the most successful quantum TST formulation is based on the isomorphism of the discretized Feynman path-integral representation of the equilibrium quantum-mechanical density operator with a classical system in which closed-ring polymers represent quantum particles.[13,14] In this approach, quantum particles are mapped onto classical closed paths $\mathbf{r}(t)$ in imaginary time t with $0\leqslant t\leqslant\beta\hbar$, where $\hbar$ is Planck's constant divided by 2π.[13] In practical implementations, discretizations of the closed paths leads to an isomorphism between the path integral formalism and a system of interacting ring polymers with P beads governed by the effective potential

$$U_{\mathrm{eff}}=\sum_{i=1}^{N}\frac{Pm_i(k_BT)^2}{2\hbar^2}\sum_{j=1}^{P}(\mathbf{r}_i^{(j)}-\mathbf{r}_i^{(j+1)})^2+\frac{1}{P}\sum_{j=1}^{P}U(\mathbf{r}_1^{(j)},\ldots,\mathbf{r}_N^{(j)}), \tag{3}$$

where N is the number of atoms which are treated quantum-mechanically, P is the number of beads in each polymer, m_i is the mass of atom i, and $\mathbf{r}_i^{(j)}$ is the position of bead j of atom i. In Eq. (3), the closure of the Feynman path is imposed by periodic boundary conditions $\mathbf{r}_i^{(j)}=\mathbf{r}_i^{(P+j)}$, and $U(\mathbf{r}_1,\ldots,\mathbf{r}_N)$ is the potential energy calculated either by *ab initio* methods or by a molecular mechanics potential. The first term in Eq. (3) describes harmonic interactions between the beads and is related to the average quantum kinetic energy. In the limit of an infinite number of beads, the discrete representation of the paths becomes exact and averages over the canonical Boltzmann distribution with effective potential U_{eff} yield the full quantum canonical ensemble averages. In practice, however, only approximately 20 beads are required for each nucleus to obtain converged quantum averages for many systems. The classical limit is recovered as the masses $m_i\rightarrow\infty$, in which case the polymer representing the quantum particle collapses onto the center-of-mass or *centroid* of the ring polymer

$$\overline{\mathbf{r}_i}=\frac{1}{P}\sum_{j=1}^{P}\mathbf{r}_i^{(j)}. \tag{4}$$

The path-integral theory has been utilized to formulate an approximate theory of quantum-activated processes using the idea that the full quantum reaction rate is governed by the activation free energy for the centroid reaction coordinate.[5] However, one cannot obtain the real time dynamical evolution of the quantum system simply by replacing the classical potential energy surface U by U_{eff} in the Hamilton equations. In practice, only static properties can be obtained within this imaginary-time path-integral approach unless methods of analytic continuation are used.[15]

B. The molecular mechanics based importance function method

In imaginary-time *ab initio* path integral simulations, sampling efficiency is extremely important as accurate electronic structure calculations for each configuration can take minutes on a modern computer. Recently, Iftimie *et al.*[6] proposed a method of improving the sampling efficiency of *ab initio* simulations. The approach, called the molecular mechanics-based importance sampling method (MMBIF), consists of utilizing an auxiliary Markov chain with a known asymptotic classical distribution to propose trial configurations for an *ab initio* based Monte Carlo simulation. In this scheme, each trial configuration is obtained as the last state in a series of classical updates starting from the current configuration in the *ab initio* simulation. The proposed configurations are then accepted or rejected in the *ab initio* chain according to the usual Metropolis–Hastings algorithm.[16–18] It has been demonstrated[6] that if the auxiliary classical potential function is a reasonably good approximation to the *ab initio* energy function, the MMBIF method reduces the integrated correlation time of a simple *ab initio* Monte Carlo simulation by two orders of magnitude.

Although the MMBIF method can be implemented for the path-integral simulation in a straightforward fashion yielding integrated correlation times which are roughly comparable to those obtained in the simulation treating the nuclei classically, importance sampling methods can be used to further reduce the integrated correlation time. In a practical implementation,[9] the efficiency of the *ab initio* path-integral

simulation can be increased by generating two coupled, non Markovian simulations in parallel, one with a limiting distribution determined by $U_{\text{eff}}^{\text{cl}}+U_c^{\text{DFT}}-U_c^{\text{cl}}$, and the second with the desired limiting Boltzmann path-integral distribution determined by $U_{\text{eff}}^{\text{DFT}}$. The effective potential energies $U_{\text{eff}}^{\text{cl}}$ and $U_{\text{eff}}^{\text{DFT}}$ are calculated via molecular mechanics and *ab initio* potentials, respectively, while U_c^{cl} and U_c^{DFT} represent the classical nuclei molecular mechanics and classical nuclei *ab initio* potentials, respectively. The superscript DFT refers to the *ab initio* method of choice for calculating the electronic energy of a structure, which in Ref. 9 was chosen to be density functional theory (DFT).

The generalization of the MMBIF method to path-integral simulation is a Monte Carlo method and, in sharp contrast to dynamical methods of sampling the effective distribution, there is no need to use sophisticated staging and thermostating methods to equilibrate the paths. Iftimie *et al.*[9] have demonstrated that if a reasonably good classical description of the *ab initio* potential is available, the MMBIF path-integral simulation method decreases the integrated correlation time of a simple DFT Markov chain path-integral simulation by at least three orders of magnitude and is significantly faster than path-integral molecular dynamics at a given level of statistical uncertainty.

C. Computational details

In order to calculate accurate centroid potentials of mean force describing the tautomerization process in malonaldehyde, a method for reliably calculating the energies of different configurations of the system must be available. Classical potentials are usually parameterized to describe only one topological arrangement of the bonds in the system generally representing a local minimum on the potential energy surface. As such, chemical reactions involving bond-breaking and bond-forming processes between different stable structures can not be realistically represented. Recently, empirical valence bond approaches[19] have been developed that interpolate between the existing descriptions of different local minima on the potential energy surface.

The correct energetics in hydrogen-bonded systems and in proton transfer reactions are difficult to describe even with *ab initio* methods. In particular, DFT studies of weak hydrogen-bonding systems have proved to be particularly difficult and only limited success has been achieved in predicting the geometries and energies for the important configurations on the potential energy surface using most exchange-correlation functionals.[20] The non-local exchange-correlation schemes developed by Proynov, Vela, and Salahub[21] have shown particular promise for the description of hydrogen-bonded systems. Sirois *et al.*[22] have demonstrated that their kinetic-energy dependent exchange functionals (BLAP and PLAP) performed better than all GGA options (BP86, PP86, PW91), BLYP, or other hybrid methods (B3LYP, B3PW91) on systems involving intramolecular hydrogen bonds, including the malonaldehyde. The predictions for equilibrium and transition state geometries as well as the energetics was in agreement with high-quality post-Hartree–Fock calculations [CCSD(T) and G2][22].

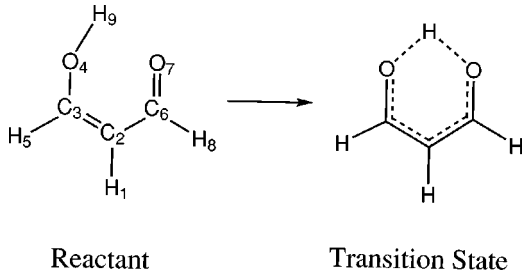

FIG. 1. The proton transfer tautomerization reaction in the enol form of malonaldehyde. The product state (not shown) is chemically equivalent to the reactant state.

The accuracy of the *ab initio* post-Hartree–Fock methods to describe the energetics of intramolecular hydrogen bonds can be tested by calculating the magnitude of the gas-phase tunneling splitting in malonaldehyde. Although several contradictory results have appeared in the literature over the years,[23] the recent calculations of Benderskii *et al.*[24] using accurate instanton methods[25] estimate the energy difference between reactant and transition state configurations (shown in Fig. 1) to be 4.3 kcal/mol. The results of these calculations are in excellent agreement with DFT calculations using the kinetic-energy dependent PLAP exchange functional, and with the more computationally-intensive CCSD(T) and G2 estimates. Moreover, the instanton study of the tunneling splitting[24] predicts an ''imaginary'' frequency at the transition state of 1290 cm^{-1}, in very good agreement with the PLAP prediction of 1270 cm^{-1} obtained in our study.

For the simulations described in the present work, the energies of different configurations were carried out using a modified version of the LCGTO-DFT program DEMON-KS3.4.[26,27] The DFT electronic structure calculations were carried out as in Ref. 22, where the application of DFT methods to hydrogen-bonding systems is discussed in detail. A double-ζ plus polarization (DZVP) orbital basis set was used for all atoms and the convergence level for the SCF (self-consistent field) energy using the auxiliary fitting basis sets[22] was 0.01 kcal/mol.

III. RESULTS

The molecular mechanics based importance function method was applied to the calculation of the *ab initio* centroid potentials of mean force describing the proton transfer reaction in the enol form of malonaldehyde depicted in Fig. 1. The molecular mechanics guiding potential described in Ref. 9 was utilized. The reaction coordinate ξ determining the potential of mean force was initially chosen to depend on the coordinates of the atoms involved in the bond-breaking and bond-forming processes,

$$\xi=\frac{d_{O_4H_9}-d_{O_7H_9}}{d_{O_4O_7}}. \tag{5}$$

In Eq. (5), d_{ij} is the distance between atoms i and j in the system if the atoms are treated classically and represents the distance between the centroids of the ring polymer path-integral representations of the atoms i and j when the nuclei are represented as paths.

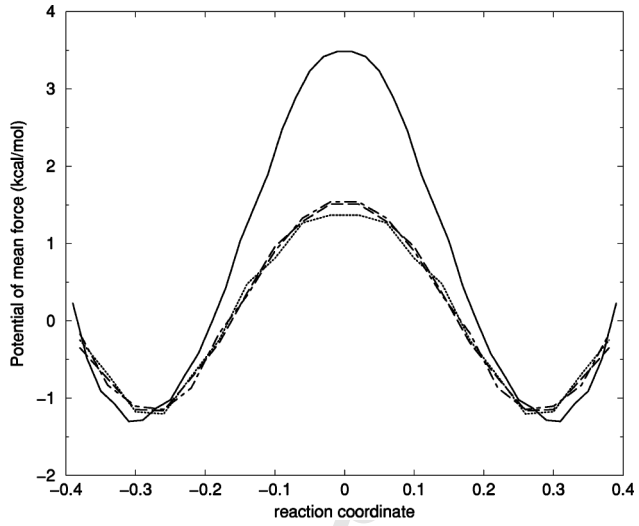

FIG. 2. The *ab initio* potential of mean force for the reaction coordinate defined in Eq. (5) at $T=300$ K. The solid lines are the results obtained with classical nuclei, the dotted–dashed line are the results with a quantized transferring proton H_9, and the long-dashed and dotted lines correspond to results with quantized H_9, O_4, O_7, and all nuclei, respectively. The reduction in the barrier height of the potential of mean force obtained by quantizing the carbon atoms in addition to H_9, O_4, and O_7 is at the limit of the statistical resolution of the simulation (0.15 kcal/mol).

All calculations of the potential of mean force include a constant factor to ensure that the configurational partition function for the reactant well is unity. This construction implies that $\exp\{-\beta\phi(\xi)\}=P(\xi)$ is the probability density for the reaction coordinate in the reactant well.

A. Quantum nuclear dispersion effects of carbon atoms on the centroid potential of mean force: *Ab initio* potential

In order to calculate the effect of the quantum dispersion of the carbon atoms on the centroid potential of mean force describing the tautomerization process in the enol form of malonaldehyde, a series of four simulations was performed. For each simulation, corresponding to different isotopic substitutions for the nuclear degrees of freedom in malonaldehyde, the potential of mean force was calculated. In the first simulation, all nuclear degrees of freedom were treated as classical point particles which, in the path-integral language, corresponds to a malonaldehyde molecule substituted with fictitious isotopes of infinite mass for all the atoms. In the next three simulations, the masses of the transferring proton, the transferring proton and the oxygen atoms, and finally the mass of all the atoms were decreased to values corresponding to the mass of their most abundant natural isotopes. The results of the four simulations in Fig. 2 show that quantization of the transferring proton leads to a decrease of 2.5 kcal/mol in the normalized potential of mean force at the transition state. Further quantization of the oxygen atoms leads to a negligible change in the potential of mean force, while additional quantization of the carbon atoms lowers the centroid potential of mean force at the dividing surface by 0.15 kcal/mol, which is roughly the magnitude of the 96% confidence interval at the transition state. The decrease in the potential of mean force at the transition state due to additional quantization of the carbon nuclear degrees of freedom can be interpreted as a secondary ''isotope'' effect in which the most abundant isotope of carbon with mass 12 amu is substituted by a massive (fictitious) isotope.

B. Centroid potential of mean force with an empirical valence bond potential

Recently, the proton transfer tautomerization reaction in the enol form of acetylacetone was studied using an empirical valence bond potential.[2] Although acetylacetone differs chemically from malonaldehyde due to the substitution of hydrogen atoms H_5 and H_8 with methyl groups, the chemical difference between acetylacetone and malonaldehyde should have minimal effect on the mechanism and rate of the proton transfer reaction.

A description of the construction of the empirical valence bond (EVB) potential for the proton transfer reaction in acetylacetone can be found in Ref. ■■. The potential energy surfaces for the reactant and product states, consisting mostly of standard bond, angle, dihedral, and nonbonded potentials, were combined into a total potential energy surface that allows a transition between the reactant and product states. The diabatic surfaces for the reactant and product states were coupled through a configuration independent constant energy term parameterized so that the energy difference between reactant and transition state configurations matched that calculated with an *ab initio* potential at the Hartree–Fock level. The electrostatic energy in the EVB potential was calculated utilizing fixed atomic charges fitted to match the Hartree–Fock charge distribution around the molecule.

The total potential energy surface for the proton transfer reaction in acetylacetone described in Ref. 19 was adapted for the study of the proton transfer reaction in the enol form of malonaldehyde. The charges on H_5 and H_8 were taken as the sum of atomic charges forming the methyl groups in acetylacetone, while the C_3–H_5 and C_6–H_8 bond vibration parameters were taken to coincide with the same parameters for the C_2–H_1 bond in acetylacetone. The adapted potential gives an energy difference of 8.75 kcal/mol between the reactant and transition state conformations, a value which is about 0.7 kcal/mol lower than that of the acetylacetone system. This difference may be due to Urey–Bradley angular potentials for certain bond angles not included in this study.

The potentials of mean force for the proton transfer process in the enol form of malonaldehyde corresponding to the same isotopic substitutions as in the DFT calculations reported in the previous section are shown in Fig. 3. The results in Fig. 3 are similar to those reported in Ref. 2 for all combinations of isotopic substitutions. Note that quantization of the proton decreases the transition state value of the potential of mean force in the EVB simulation by approximately 2 kcal/mol, in rough agreement with the *ab initio* results. However there are important differences between the EVB and *ab initio* simulations with respect to the centroid potential of mean force. As is evident in Fig. 3, quantization of the carbon nuclei leads to a further decrease in the centroid potential of mean force value at the dividing surface by approximately 0.8 kcal/mol in the EVB simulation, whereas

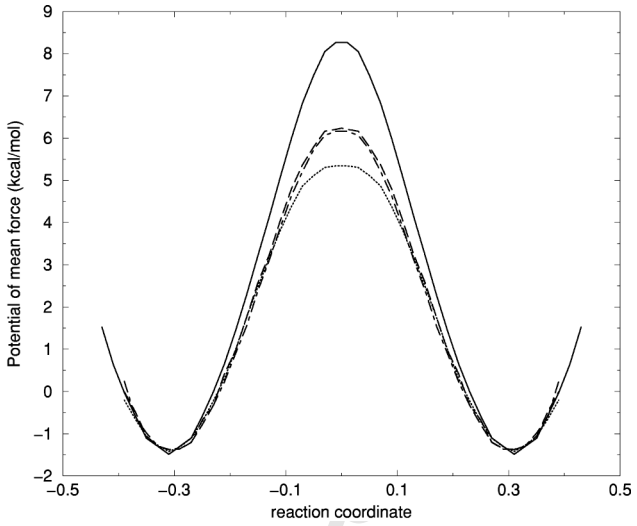

FIG. 3. The potential of mean force calculated from the EVB simulation under the same conditions and with the same labeling of isotopic substitutions as in Fig. 2. The statistical uncertainties for all curves are less than 0.15 kcal/mol for the relevant regions of the reaction coordinate. Note the quantization of the carbon atoms leads to an additional drop in the barrier of roughly 0.8 kcal/mol.

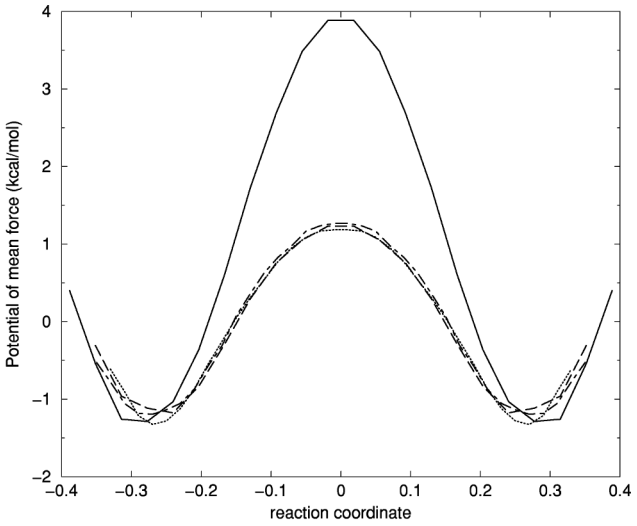

FIG. 4. The potential of mean force calculated from the bond evolution theory simulations under the same conditions and with the same labeling as in Fig. 2. The statistical uncertainties in all simulations are approximately 0.1 kcal/mol in the reactant and transition state regions.

a much smaller (and possibly statistically insignificant) decrease of about 0.15 kcal/mol is observed in the *ab initio* calculations.

In order to investigate the origin of the difference between the *ab initio* and the EVB potentials of mean force in more detail, another series of calculations was performed. First, the EVB potential of mean force for the proton transfer reaction with quantization of just the nuclear degrees of freedom representing the carbon atoms C_3 and C_6 was calculated. No difference in the EVB potential of mean force value at the transition state was determined between treating only the carbon atoms degrees of freedom quantum-mechanically and treating all atoms classically. However, when the nuclear degrees of freedom of the carbon atoms C_3 and C_6 as well as those of the transferring proton H_9 were treated quantum-mechanically, all the nuclear quantum effects in the EVB potential of mean force were recovered. To assess how the secondary atom quantization effects influence the centroid potential of mean force when the mass of the primary atom changes, another series of simulations was performed. In these simulations, the mass of deuterium and tritium were utilized for the transferring proton, while the nuclear degrees of freedom of the carbon atoms C_3 and C_6 were treated classically as well as quantum mechanically. The results of these simulations indicate that the secondary isotope effects decrease for the EVB system as the mass of the primary particle increases.

C. Centroid potential of mean force with the molecular mechanics guiding potential

In order to elucidate the origin of the influence of the quantum nuclear degrees of freedom of secondary atoms on the centroid potential of mean force, it is helpful to compare the importance of quantization of carbon nuclear degrees of freedom in the EVB system with the those in a molecular mechanics potential created by a different scheme. For the purposes of comparison, we have chosen to utilize the molecular mechanics created in the MMBIF method guiding the DFT simulation.

The bond evolution theory principles used in the construction of the molecular mechanics guiding potential have been described in detail in Ref. 9. The potential was constructed as the sum of two terms. The first term consisted of a double-well potential depending on a control parameter η which is a function of only the coordinates of the atoms directly involved in the bond-breaking and bond-forming processes. The second term consisted of a sum of harmonic potentials taken to depend parametrically on η. The second type of potentials describe the evolution of the bond, bond angle and dihedral motions during the reaction.

In Fig. 4, the centroid potential of mean force calculated from simulations based on the bond evolution theory molecular mechanics potential is plotted as a function of the reaction coordinate for a number of isotopic combinations. The results for the potential of mean force obtained from the simulation based on the bond evolution theory molecular mechanics guidance potential are virtually indistinguishable from the *ab initio* results shown in Fig. 2. Specifically, the path integral treatment of the proton degrees of freedom decreases the potential of mean force value at the transition state by approximately 2.5 kcal/mol, while a marginally significant further decrease in the potential of mean force of 0.1 kcal/mol is obtained when the oxygen atoms are ''quantized.'' In contrast to the EVB simulations, the quantum dispersion of the carbon nuclei leads only to a decrease in the potential of mean force at the transition state of 0.1 kcal/mol, which is the limit of the statistical resolution of the simulation. Given that the EVB and bond evolution theory potentials predict quite different isotope effects on the centroid potential of mean force, subtle differences must exist in the reaction mechanisms predicted by the two molecular mechanics potentials. In particular, the dependence of the sec-

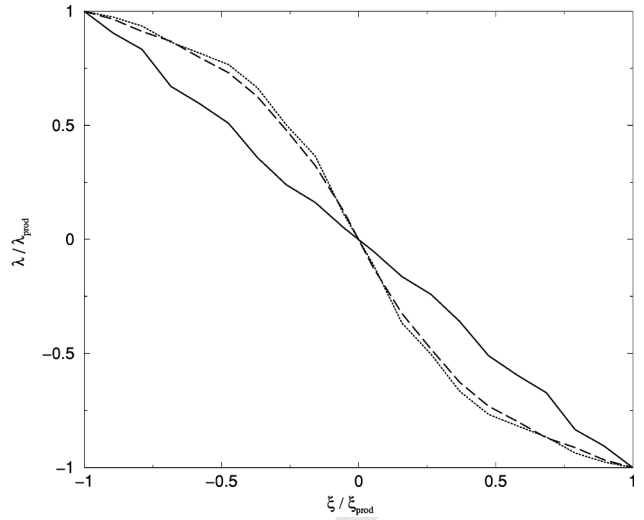

FIG. 5. A plot of the maximum density of points in the (ξ,λ) plane from the EVB (dotted line), bond evolution theory (solid line), and modified bond evolution theory (dashed line) simulations. ξ is the reaction coordinate defined in Eq. (5), and $\lambda = d_{C_3O_4} - d_{C_6O_7}$ is the difference between the carbonyl and enolic bond lengths. ξ_{prod} and λ_{prod} represent the ξ and λ values calculated for the product configurations.

ondary atom isotope effects on the mass of transferring proton obtained with the EVB potential suggests that the coupling between the proton and heavy atom motions could be described differently in the two potentials.

A useful way of probing the nature of the coupling between the reaction coordinate and the position of the carbon atoms is to examine scatter plots from the simulations of ξ and a variable depending on the position of the carbon atoms. If we denote $\lambda = d_{C_3O_4} - d_{C_6O_7}$ to be the difference between the carbonyl and the enolic bond lengths during the reaction, a plot of the maximum density of points in a scatter plot of ξ and λ (see Fig. 5) illustrates the qualitative difference in the coupling of heavy and light atoms in the EVB and bond evolution potential simulations. In the case of the bond evolution theory simulations, the curve describing the trajectory of the maximum density of points in the (ξ,λ) plane as the reaction proceeds is a straight line. In the case of the EVB simulations, however, the same trajectory has a hyperbolic tangent profile suggesting that the path of maximum reaction probability on the EVB potential energy surface has a substantially enhanced projection onto ξ at the beginning of the reaction and has an increased projection onto λ in the neighborhood of the dividing surface compared to the trajectory for the bond evolution theory potential.

In the bond evolution theory potential, the bond vibration potentials describing the evolution of the carbonylic, C_3–O_4, and enolic, C_6–O_7 bonds during the proton transfer reaction are of the form[9]

$$V_{CO} = k(\xi)(d_{CO} - d^{eq}(\xi))^2, \tag{6}$$

where the force constant $k(\xi)$ depends linearly on the reaction coordinate interpolating between its value in the reactant and transition state configurations. The equilibrium bond length $d^{eq}(\xi)$ in the potential depends parametrically on ξ and interpolates parabolically between values in the reactant, transition state and product regions. In the bond evolution theory potential, the equilibrium C–O bond lengths $d^{eq}(\xi)$ can be obtained by an energy minimization procedure with the control parameter ξ fixed. The linear shape of the projection of the path of maximum reaction probability (maximum density of points) in the (ξ,λ) plane is due to the fact that the bond lengths in the transition state are almost half the sum of their values in reactant and product configurations.

In order to verify if the departure from linearity of the projection in the (ξ,λ) plane of the path of maximum reaction probability can give rise to inflated isotope effects due to the secondary atoms, a modified bond evolution theory potential was constructed in which $d^{eq}(\xi)$ assumed a hyperbolic tangent form with respect to ξ (see Fig. 5). In the simulations with this modified potential, a significant increase in the importance of the nuclear dispersion of the carbon degrees of freedom was obtained utilizing the hyperbolic tangent over the linear profile for $d^{eq}(\xi)$. More precisely, the secondary isotope effect obtained by quantization of the carbon atoms in addition to quantization of the transferring proton resulted in a decrease in the centroid potential of mean force at the transition state of 0.4 kcal/mol. The difference in the potential of mean force for the linear versus hyperbolic profile supports the hypothesis that the functional form of the projection in the (ξ,λ) plane of the path of the maximum reaction probability has an important influence on the magnitude of the secondary atom tunneling contribution to the centroid potential of mean force. Direct modification of the EVB potential surface to control the synchronous reorganization of the backbone skeleton as the control parameter ξ changes along the path of maximum reaction probability is challenging to implement. In fact, it is very difficult to enforce a particular reaction mechanism in the EVB construction of the reaction surface because the reaction mechanism is sensitively dependent on the off-diagonal coupling term coupling the diabatic states for the reactant and product configurations.

It is intriguing that the quantization of only the carbon atoms C_3 and C_6 has a significant influence on the magnitude of the secondary isotope effects obtained with the EVB potential. Because λ depends on the position of the carbon as well as of the oxygen nuclei, the departure from linearity of the path of maximum reaction probability suggests that the carbon as well as the oxygen atoms should be important in the isotope effects. Furthermore, other choices of λ which depend on the nuclear position of the carbon atom C_2 give similar scatter plots indicating that this atom should also contribute to the secondary isotope effects. The favored role of the carbon atoms C_3 and C_6 in the secondary isotope effects is currently being investigated.

D. Centroid potential of mean force and kinetic isotope effects

When unimolecular reaction rate descriptions of proton transfers are valid, the centroid potential of mean force can be used to estimate quantum rate constants. Under these conditions, it is important to assess the accuracy of the centroid TST approximations to the true quantum rates. The accuracy of centroid transition state theory in predicting quantum re-

TABLE I. 96% confidence intervals for centroid transition state rate constants using the EVB potential.

Reaction coordinate	Isotopic substitution	^{1}H	^{2}H	^{3}H
ξ_1	^{12}C	$5.55\cdots7.42\times10^8$	$5.39\cdots7.12\times10^7$	$2.07\cdots2.6\times10^7$
	^{100}C	$1.41\cdots1.88\times10^8$	$1.73\cdots2.44\times10^7$	$1.17\cdots1.51\times10^7$
ξ_2	^{12}C	$5.49\cdots7.37\times10^8$	$4.89\cdots6.46\times10^7$	$2.22\cdots2.82\times10^7$
	^{100}C	$1.43\cdots1.91\times10^8$	$1.91\cdots2.67\times10^7$	$1.15\cdots1.48\times10^7$
ξ_3	^{12}C	$5.1\cdots6.81\times10^8$	$6.11\cdots10.5\times10^7$	$2.96\cdots4.46\times10^7$
	^{100}C	$1.26\cdots1.93\times10^8$	$2.29\cdots3.6\times10^7$	$1.86\cdots2.69\times10^7$

action rates depends substantially on the temperature at which the reaction takes place. It has been demonstrated that centroid transition state theory becomes identical to classical transition state theory for condensed phase systems in the high-temperature approximation[4,5] when all particles behave classically. Furthermore, studies of reaction rates using unbounded one-dimensional potentials have shown that the centroid transition state theory works well for transitions involving symmetric barriers[5,28] for all temperatures. Although centroid TST often fails for asymmetric transitions for unbounded one-dimensional potentials in the low-temperature (tunneling) regime, no significant departures from results calculated using exact quantum theory have been observed in the high, intermediate (semiclassical), or in the crossover intervals of temperature.[29–32] For one-dimensional potentials with a parabolic barrier, the crossover temperature between the low temperature (tunneling) and the intermediate (semiclassical) regimes in the absence of any dissipation is given by

$$T_{\mathrm{cr}}=\frac{\hbar\omega^{\mathrm{TS}}}{2\pi k_B}, \tag{7}$$

where ω^{TS} is the ''imaginary'' frequency calculated at the transition state.[33] In the general multidimensional case, the crossover temperature can be approximated by considering the tunneling process as one-dimensional in an effective potential whose barrier frequency is equal to the imaginary frequency calculated at the multidimensional transition state geometry. This approximation suggests that reactions at room temperature are dominated by quantum corrections to thermal hopping[10] if the imaginary frequency is roughly below 1400 cm^{-1}. This condition on the magnitude of the barrier frequency can be taken as an approximate upper bound for using variational centroid TST methods to estimate quantum rate constants at room temperature.

An important decision in the study of chemical reactions is the choice of a reaction coordinate. In classical mechanics, it has been demonstrated that TST provides an upper limit for the true chemical reaction rate.[34] For a good choice of reaction coordinate, the re-crossing factor is near unity and can be neglected. In practice, the variational bound of TST rate constants is often implemented by approximating the true reaction rate by the smallest TST rate obtained for different choices of reaction coordinate.[35] The advantage of such an approach is that the potential of mean force is a static correlation function that can be obtained without simulating the true dynamics of the system. However, as there is no variational bound theorem for the centroid transition state approximation to the full quantum rate, the selection of the best reaction coordinate is much more difficult in a quantum context than in a classical context. Until an exact theory for the dynamical recrossing factor appropriate for centroid transition state theory is formulated, the question of which reaction coordinate gives the best centroid TST estimate to the true quantum rate cannot be resolved.

In order to assess the sensitivity of the centroid potential of mean force results to the choice of reaction coordinate, all the potentials of mean force obtained in the previous sections have been recalculated using a reaction coordinate depending on the positions of the primary as well as on the secondary atoms. In addition, two other reaction coordinates were investigated. First, to compare the reaction rates estimated in this study using the EVB potential with similar results obtained in the tautomerization of acetylacetone from Ref. 2, the reaction coordinate ξ_2 was used, where ξ_2 is given by

$$\xi_2=\left(\mathbf{r}_{\mathrm{H}_9}-\frac{\mathbf{r}_{\mathrm{O}_4}+\mathbf{r}_{\mathrm{O}_7}}{2}\right)\frac{\mathbf{r}_{\mathrm{O}_4}-\mathbf{r}_{\mathrm{O}_7}}{||\mathbf{r}_{\mathrm{O}_4}-\mathbf{r}_{\mathrm{O}_7}||}. \tag{8}$$

Finally, the reaction coordinate

$$\xi_3=0.4\xi_1-\frac{\lambda}{d_0}, \tag{9}$$

where $\lambda=d_{\mathrm{C_3O_4}}-d_{\mathrm{C_6O_7}}$ is the control parameter introduced previously and $d_0=1$ Å is a scaling length to make the reaction coordinate dimensionless. Note that ξ_3 depends on coordinates of both primary and secondary atoms. The form of Eq. (9) is determined by the best linear combination of the variables ξ_1 and λ/d_0 which approximates the projection of the path of maximum reaction probability in the $(\xi_1,\lambda/d_0)$ plane.

Table I summarizes the estimated 96% confidence intervals for reaction rates calculated within the centroid transition state theory framework for the EVB potential. In all calculations the quantum degrees of freedom of all nuclei were represented in the imaginary-time path-integral formalism by closed-ring polymer beads, except for the simulations corresponding to the rows with ^{100}C where the carbon atoms C_3 and C_6 were treated as point particles. Treating the carbon atoms as point particles is equivalent in the path-integral language to studying reaction rates in a malonaldehyde molecule labeled at the two carbon centers with very heavy isotopes, here taken to have a mass of 100 amu. In addition, in cases where the carbon atoms were treated as point particles,

the mass of 100 amu was used for the carbon atoms in the calculation of the effective mass prefactor given in Eq. (2). In all calculations the most naturally abundant isotopes were used for the oxygen atoms O_4 and O_7, the hydrogen atoms H_1, H_5 and H_8, and for the carbon atom C_2 while isotopes ^1H, ^2H, and ^3H were used for the transferring proton. As can be seen in Table I, the secondary kinetic isotope effect predicted with centroid transition state theory depends significantly on the mass of the transferring proton for all reaction coordinates considered.

E. Secondary kinetic isotope effects depending on the mass of the primary particle and secondary atom tunneling effects

Semiclassical transition state theory[10,36] can provide valuable insight into the nature of secondary kinetic isotope effects whose magnitude depends on the mass of the primary particle. Semiclassical transition state theory assumes that several energy levels lie below the top of the barrier separating the reactant and product subspaces of configuration space and that the transfer over the barrier is described by *classical* dynamics. As a consequence, tunneling effects due to the quantum nature of the dynamics at the top of the barrier are neglected in semiclassical TST. However, zero-point vibration terms are incorporated in an approximate fashion in which the anharmonicity of vibrations and coupling between normal modes are usually neglected.[36,37] Under these conditions, the reaction rate is found to depend only on the (classical) barrier height of the reaction and on the vibrational frequencies calculated in the reactant and transition state configurations. Provided the semiclassical TST approximations are valid and tunneling contributions to the reaction rate are relatively small, in the limit of high-temperature where the parameter $u=\hbar\omega/k_BT\leqslant 2$ for all the frequencies ω of the normal modes in the equilibrium and transition state configurations, it can be shown that the following equation is obeyed[38]

$$\ln\frac{k^{(p,s)}}{k^{(p,s')}}=\ln\frac{k^{(p',s)}}{k^{(p',s')}}, \tag{10}$$

where $k^{(p,s)}$ is the rate constant when the primary and secondary atoms are in their most abundant isotopic forms p and s. In this notation, the rate constant $k^{(p',s)}$ corresponds to the rate of proton transfer when isotopic substitutions have been made for the primary atoms alone. Equation (10) is known as the rule of geometric mean,[39] which states that the mass of primary atoms does not modify the magnitude of secondary kinetic isotope effects and vice versa. Although the rule of geometric mean was originally derived in the high temperature limit in which $\hbar\omega\leqslant 2k_BT$, experiments have established that the range of validity of the rule extends to intermediate temperatures.[38] Semiclassical TST calculations for rate constant calculations based on simplified models have consistently reported negligible deviations from the rule of geometric mean.[37] However, when tunneling contributions are incorporated in an approximate fashion by multiplying the semiclassical TST reaction rates by the truncated Bell's tunneling correction factor[36] c, where

$$c=\frac{u^{\ddagger}}{2\sin(u^{\ddagger}/2)}, \tag{11}$$

significant departures from the rule of geometric mean have been observed for several systems.[39] In Eq. (11), $u^{\ddagger}=\hbar\omega^{\ddagger}/k_BT$ and $\omega^{\ddagger}$ is the imaginary frequency calculated at the transition state configuration. It should be noted that only moderate tunneling contributions can be calculated with Eq. (11) since this equation requires that $u^{\ddagger}<2\pi$, or, equivalently, that the temperature T is in the thermal hopping and quantum corrections regime above T_{cr}.[10] These findings have been generalized in the physical organic chemistry literature in which significant deviations from the rule of geometric mean are interpreted as an indication of tunneling for both the primary and secondary atoms.[37,39]

As can be seen in Table *I*, centroid transition state theory predicts kinetic isotope effects which do not obey the rule of geometric mean for the malonaldehyde system described by the EVB potential. Indeed, in the EVB simulations it was observed that the decrease of the potential of mean force for the proton transfer reaction due to the quantization of the heavy atoms depends on the mass of the proton. Calculations were carried out to estimate the zero point energy contributions to the rate constant by computing the vibrational frequencies in the reactant and transition state configurations. Using the calculated EVB reactant and transition state frequencies to estimate the zero-point vibration effects from primary and secondary atoms in the semiclassical TST approximation, it is apparent that the rule of geometric mean (10) is satisfied. This therefore suggests that zero-point vibrations alone are unlikely to account for the secondary isotope effects observed with the EVB potential, even when more accurate methods which include vibrational anharmonicities and mode coupling are utilized to estimate the zero-point vibration effects.

The parameter r, where r is defined to be

$$r=\ln\frac{k^{(p,s)}}{k^{(p,s')}}\Big/\ln\frac{k^{(p',s)}}{k^{(p',s')}}, \tag{12}$$

is often used in the physical organic chemistry literature as a quantitative measure of the extent of breakdown of the rule of geometric mean. Figure 6 displays the probability of the estimated value of r calculated using the data in Table I for primary atom isotopes ^1H and ^3H and secondary atom isotopes ^{12}C and ^{100}C. Care should be exercised to avoid overinterpretation of the results in Table I and Fig. 6. As can be seen in Table I and Fig. 6, different choices of reaction coordinate yield slightly different results for individual kinetic isotope effects and the probability density of r defined in Eq. (12). As no information concerning recrossing factors for the three choices of reaction coordinate is available, it is difficult to assess which particular reaction coordinate provides a better estimate of the real isotope effects. Although some researchers believe that a lower quantum centroid TST rate indicates a better choice of the dividing surface,[2,5] in the absence of an exact variational principle requiring recrossing factors to be smaller than unity in quantum centroid transition state theory, there is little evidence to suggest a preferred

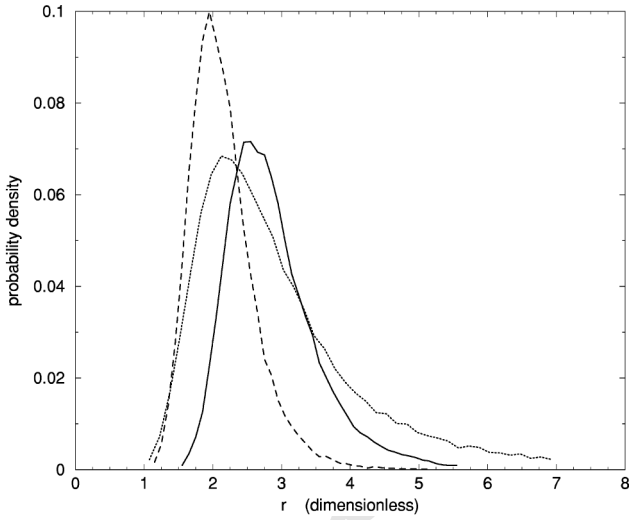

FIG. 6. The probability density for r defined in Eq. (12) using primary isotopes ^{1}H and ^{3}H and secondary isotopes ^{12}C and ^{100}C. The skewed probability densities are obtained using the probability densities for the reaction rates in Table I. The solid line corresponds to reaction coordinate ξ, and the dashed and dotted lines correspond to ξ_2 and ξ_3, respectively.

reaction coordinate choice, particularly since the reaction coordinates result in overlapping confidence intervals for most reaction rates. One can perhaps view the inability to identify a preferred reaction coordinate as leading to a broader (nonnormal) probability density of possible values of r described by the envelope of the three distributions in Fig. 6. Although it is likely that the envelope of the three distributions in Fig. 6 is a conservative estimate of the uncertainty in r, the envelope of the probability density in r has negligible area in the semiclassical TST region $r=1$. This result implies that the breakdown of the rule of geometric mean calculated by centroid TST is likely to be valid for any reasonable choice of reaction coordinate and strongly suggests the rule of geometric mean does not hold when exact dynamical methods are used to calculate reaction rates. The breakdown of the rule of geometric mean suggests that tunneling of the carbon atoms is an important component of the reaction mechanism in the EVB study of the tautomerization process in the malonaldehyde ''core,'' and is likely to be important in proton transfer reactions in which secondary kinetic isotope effects are found to depend on the mass of the transferring proton.

IV. DISCUSSION AND CONCLUSIONS

In this article the origin and magnitude of centroid TST calculations of secondary isotope effects in intramolecular proton transfer reactions have been investigated for molecular mechanics and *ab initio* potentials. The core region of the transfer process was modeled to have the chemical topology of malonaldehyde for which very accurate *ab initio* centroid TST calculations are possible. It was demonstrated that potential energy terms coupling the motion of the transferring proton with the motion of secondary atoms can induce a breakdown of the rule of geometric mean predicted using imaginary-time path-integral calculations. Such a scenario arises in the proton transfer reaction in malonaldehyde described by an empirical valence bond potential. In the EVB system, the magnitude of the secondary isotope effect on the potential of mean force was found to vary significantly with the mass of the transferring proton. When unimolecular centroid TST rate descriptions are appropriate, this variation suggests the mass of the primary atom influences the magnitude of secondary kinetic isotope effects, a phenomenon which is considered to be a signature of secondary atom tunneling effects in the physical organic chemistry literature.[39]

Significant tunneling contributions to secondary kinetic isotope effects have been demonstrated to be important in several reactions,[37] including some occurring in biochemical systems such as alcohol dehydrogenase enzymatic reactions.[40–42] In these systems, the tunneling contributions to secondary kinetic isotope effects have been interpreted using simplified models of the potential energy surface and Bell's treatment of the tunneling effect.[36,37,39] In these studies, an increased secondary atom contribution to the negative eigenvalue of the Hessian of the mass-weighted potential energy calculated at the transition state configuration is believed to account for the increase in the dependence on the mass of the secondary atoms of the tunneling corrections. As these considerations are not dependent on the details of any specific model, the predictions are likely to be correct in a qualitative sense and offer an *a posteriori* explanation for many of the experimental results where the breakdown of the rule of geometric mean is observed. However, the use of simplified models and the approximate treatment of tunneling effects in the Refs. 37 and 39 precludes any accurate prediction of secondary kinetic isotope effects. More accurate calculations could be based upon realistic molecular mechanics potentials which describe chemical events in combination with centroid quantum transition state theory methods. Such calculations have been carried out by Hinsen and Roux[2] via computation of the EVB centroid potential of mean force for the proton transfer process in the enol form of acetylacetone. In their study, Hinsen and Roux[2] reported a substantial contribution of the quantum dispersion of the nuclear carbon degrees of freedom to the barrier height in centroid potential of mean force. In the present article, the potential energy terms responsible for inducing significant tunneling contributions to secondary carbon isotope effects on the potential of mean force were analyzed utilizing an empirical valence bond potential adapted to describe the proton transfer reaction in malonaldehyde. Several factors were found to significantly influence the magnitude of the isotope effects on the potential of mean force in a proton transfer reaction where the motion of the primary atom is coupled to the motion of secondary atoms. First, important tunneling contributions to secondary isotope effects are expected if the motion of the secondary atoms is significantly more pronounced in the neighborhood of the transition state surface than in the reactant well. Second, a increase in the mass of the primary atom also decreases the magnitude of the tunneling contribution to the secondary isotope effects.

In contrast to the results based upon the EVB potential, when an accurate *ab initio* electronic structure calculation method based on density functional theory with a PLAP exchange functional is used for the core proton transfer region,

the quantum effects of the heavy nuclear degrees of freedom have only a marginal statistical significance, contributing to at most 0.2 kcal/mol to the total decrease in the centroid potential of mean force at the transition state. It was shown using the bond evolution theory potential that this difference could be attributed to a smaller projection in the transition state region of the most probable reaction path onto motions of the carbon skeletal atoms. Our results appear to be in moderate disagreement with a very recent *ab initio* path-integral study of the same system by Tuckerman and Marx[43] in which the quantum dispersion of the nuclei of secondary atoms lead to a decrease of roughly 0.4 kcal/mol in the *barrier height* of the centroid potential of mean force. Direct comparison between the two studies is complicated by several factors. First, although different degrees of quantization can alter the barrier height of the centroid potential of mean force, nuclear quantization can also induce simultaneous modifications in the curvature of the potential of mean force in the reactant region. The curvature plays an important role in transition state theory calculations and can, in principle, entirely compensate for changes in the barrier height of the potential of mean force. Examination of Fig. 2 in Ref. 43 suggests that quantizing the carbon atoms leads not only to a lowering of the potential of mean force barrier height but also to a broadening of the reactant well which effectively diminishes the importance of the nuclear dispersion of the secondary atoms. As no detailed statistical analysis was presented in Ref. 43, it is not clear whether the results presented there differ significantly those obtained in the present study. In addition, the study in Ref. 43 was based upon a different exchange correlation functional which yields a transition state energy barrier which is lower in energy by roughly 1 kcal/mol from that obtained with the PLAP functional. Although it may be plausible that the kinetic-energy dependent PLAP functional used in the present study provides a more accurate centroid potential of mean force and transition state theory reaction rates, secondary kinetic isotope effects depend sensitively on detailed features of the coupling between primary and secondary atom motions. Because secondary kinetic isotope effects strongly reflect the reaction mechanism and therefore details of the potential energy surface, any theoretical analysis of these effects is greatly model dependent. Given the advantage of using molecular mechanics potentials to describe chemical reactions, molecular mechanics potentials will continue to be the preferred choice of energy calculations in large molecules. Our results suggest that great care should be exercised when constructing classical potentials by fitting parameters from an *accurate* electronic structure method. In particular, the features used as fitting criteria should include the projection of the intrinsic reaction path onto important variables describing the motion of secondary atoms strongly coupled to the primary atom. Further examination of the suitability of *ab initio* methods to predict secondary kinetic isotope effects and reaction mechanism in situations where kinetic isotope effects have been experimentally determined is necessary.

Important tunneling contributions to the secondary isotope effects signify that appreciable differences in reaction rate calculations could be obtained if the nuclear degrees of freedom of the secondary atoms are not treated quantum-mechanically. In particular, when calculating proton transfer reaction rates, the nuclear degrees of freedom of the secondary atoms which are coupled significantly with the motion of the primary atom should be treated quantum mechanically. These findings have important implications to the way in which path-integral calculations of reactive processes are designed.

ACKNOWLEDGMENTS

The authors would like to thank Dennis Salahub for providing the DEMON computational package, and Sheldon Opps for reading the manuscript. This work was supported by a grant from the National Science and Engineering Research Council of Canada. R. I. would also like to thank the Ontario Ministry of Education for financial support. This work was supported by a grant from the National Science and Engineering Research Council of Canada.

[1] See, for example, E. Buncel and W. H. Saunders, Jr., *Isotopes in Organic Chemistry* (Elsevier, New York, 1992), Vol. 8, *ibid.* (Elsevier, New York, 1987), Vol. 7.
[2] K. Hinsen and B. Roux, J. Chem. Phys. **106**, 3567 (1997).
[3] S. L. Baughcum, R. W. Duerst, W. F. Rowe, Z. Smith, and E. B. Wilson, J. Am. Chem. Soc. **103**, 6296 (1981).
[4] M. J. Gillan, J. Phys. C **20**, 3621 (1987).
[5] G. A. Voth, D. Chandler, and W. Miller, J. Chem. Phys. **91**, 7749 (1989); G. A. Voth, J. Phys. Chem. **97**, 8365 (1993).
[6] R. Iftimie, D. Salahub, D. Wei, and J. Schofield, J. Chem. Phys. **113**, 4852 (2000).
[7] A. Warshel and R. M. Weiss, J. Am. Chem. Soc. **102**, 6218 (1980).
[8] X. Krokidis, V. Goncalves, A. Savin, and B. Silvi, J. Phys. Chem. A **102**, 5065 (1998); B. Silvi and A. Savin, Nature (London) **371**, 683 (1994).
[9] R. Iftimie and J. Schofield, J. Chem. Phys. **114**, 6763 (2001).
[10] P. Hänggi, P. Talkner, and M. Borkovec, Rev. Mod. Phys. **62**, 251 (1990).
[11] R. Kapral, S. Consta and L. McWhirter, in *Classical and Quantum Dynamics in Condensed Phase Simulations*, edited by B. J. Berne, G. Ciccotti, and D. F. Coker (World Scientific, Singapore, 1998).
[12] D. G. Truhlar, B. C. Garrett, and S. J. Klippenstein, J. Chem. Phys. **100**, 12771 (1996).
[13] R. P. Feynman and A. R. Hibbs, *Quantum Mechanics and Path Integrals* (McGraw–Hill, New York, 1965).
[14] D. Chandler, *Introduction to Modern Statistical Mechanics* (Elsevier, New York, 1991).
[15] G. Krilov, E. Kim, and B. J. Berne, J. Chem. Phys. **114**, 1075 (2001).
[16] G. S. Fishman, *Monte Carlo* (Springer, New York, 1996).
[17] *Markov Chain Monte Carlo in Practice*, edited by W. R. Gilks, S. Richardson, and D. J. Spiegelhater (Chapmann and Hall, London, 1996).
[18] P. Bratley, B. L. Fox, and L. E. Schrage, *A Guide to Simulation* (Springer, New York, 1987).
[19] K. Hinsen and B. Roux, J. Comput. Chem. **18**, 368 (1997).
[20] V. Barone and C. Adamo, J. Chem. Phys. **105**, 11007 (1996).
[21] E. I. Proynov, , and D. R. Salahub, Chem. Phys. Lett. **230**, 419 (1994); **234**, 462(E) (1995).
[22] S. Sirois, E. I. Proynov, D. T. Nguyen, and D. R. Salahub, J. Chem. Phys. **107**, 6770 (1997).
[23] Z. Smedarchina, W. Siebrand, and M. Z. Zgierski, J. Chem. Phys. **103**, 5326 (1995).
[24] V. A. Benderskii, E. V. Vetoshkin, J. S. Irgibaeva, and H. P. Trommsdorff, Chem. Phys. **262**, 393 (2000).
[25] V. A. Benderskii, E. V. Vetoshkin, L. von Laue, and H. P. Trommsdorff, Chem. Phys. **219**, 119 (1997).
[26] E. I. Proynov, S. Sirois, and D. R. Salahub, Int. J. Quantum Chem. **64**, 427 (1997).
[27] For details on the DEMON quantum chemistry package, see http://www.cerca.umontreal.ca/deMon/Welcom_f.html
[28] J. Lobaugh and G. A. Voth, J. Chem. Phys. **100**, 3039 (1994).
[29] G. Mills, G. K. Schenter, D. E. Makarov and H. Jonsson in *Classical and Quantum Dynamics in Condensed Phase Simulations*, edited by B. J.

Berne, G. Ciccotti, and D. F. Coker, (World Scientific, Singapore, 1998).
[30] D. E. Makarov and M. Topaler, Phys. Rev. E **52**, 178 (1995).
[31] M. Messina, G. K. Schenter, and B. C. Garrett, J. Chem. Phys. **103**, 3340 (1995).
[32] M. Messina, G. K. Schenter, and B. C. Garrett, J. Chem. Phys. **98**, 8525 (1993); , **99**, 8644 (1993).
[33] V. A. Benderskii, D. E. Makarov, and C. A. Wright, Adv. Chem. Phys. **88**, 1 (1994).
[34] D. Chandler, J. Chem. Phys. **68**, 2959 (1978).
[35] D. Chandler, in *Classical and Quantum Dynamics in Condensed Phase Simulations*, edited by B. J. Berne, G. Ciccotti, and D. F. Coker (World Scientific, Singapore, 1998).
[36] R. P. Bell, *The Proton in Chemistry*, 2nd ed. (Chapman and Hall, London, 1973).
[37] W. H. Saunders, Jr., J. Am. Chem. Soc. **107**, 164 (1985), and references therein.
[38] J. Biegeleisen, J. Chem. Phys. **23**, 2264 (1955).
[39] J. Ricker and J. Klinman, J. Am. Chem. Soc. **121**, 1997 (2001).
[40] A. Kohen, R. Cannio, S. Bartolucci, and J. P. Klinman, Nature (London) **399**, 496 (1999).
[41] B. J. Bahnson, T. D. Colby, J. K. Chin, B. M. Goldstein, and J. P. Klinman, Proc. Natl. Acad. Sci. U.S.A. **94**, 12797 (1997).
[42] Y. Cha, C. J. Murray, and J. P. Klinman, Science **243**, 1325 (1989).
[43] M. E. Tuckerman and D. E. Marx, Phys. Rev. Lett. **86**, 4946 (2001).